Journal of Structural Geology 33 (2011) 1206–1217

Contents lists available at ScienceDirect

Journal of Structural Geology

journal homepage: www.elsevier.com/locate/jsg

A deformation partitioning approach to resolving the sequence of fold events and the orientations in which they formed across multiply deformed large-scale regions

T.H. Bell*, I.V. Sanislav

School of Earth and Environmental Science, James Cook University, Townsville, Qld 4811, Australia

A R T I C L E I N F O

Article history:
Received 4 October 2010
Received in revised form
19 February 2011
Accepted 31 March 2011
Available online 20 April 2011

Keywords:
Foliation development
Porphyroblast growth
Structural development
FIAs

A B S T R A C T

Regional distributions of axial plane trends retain information on the orientation in which successive generations formed because multi-scale partitioning results in most orogenic belts preserving subsequently undeformed portions of all large-scale folds. At depths greater than ~10 km within orogens, successions of regional folds are accompanied by the sequential development of crenulation hinges in pelites, which are commonly overgrown early during their development by successive generations of porphyroblasts. Consequently, the original trends of the axial planes of these folds are preserved within the distribution of foliation inflection/intersection axes within porphyroblasts (FIAs). Peaks in the distribution of FIA trends in western Maine predominantly coincide with peaks in the distribution of trends of the axial planes of macroscopic and regional folds. The WNW–ESE (~420 Ma), N–S (408 ± 10 Ma), W–E (388 ± 9 Ma), WSW–ENE (372 ± 5 Ma), SW–NE (353 ± 4 Ma) succession of FIA peaks defines the sequence of folds and accords with map scale overprinting relationships. This quantitative approach to interpreting fold successions in multiply deformed terrains resolves timing where overprinting criteria are rare, uncertain or obliterated by younger events in portions of the orogen. Significantly, lengthy detailed histories of structural development can be extracted from a small area containing porphyroblastic rocks and applied to very large-scale regions.

1. Introduction

Resolving the succession of folds in gneiss terrains is problematical because axial plane foliations, which provide significant timing criteria, are not common in gneissic rocks (Passchier et al., 1990). Furthermore, resolving successions of folds on regional geologic maps or across a larger-scale region is commonly very difficult in multiply deformed terrains even after years of detailed mapping. For example, conflicts in interpreting the timing of fold events across the Mount Isa province have continued for more than 20 years (e.g., Bell, 1983, 1991; Loosveld, 1989; Loosveld and Etheridge, 1990; Bell and Hickey, 1998; Sayab, 2005, 2006).

A fundamental trait of deformation in natural rock is the role of deformation partitioning. It results in the local preservation of complex geometries that many geologists find difficult to resolve and which can be dismissed or rationalized as perturbations in the flow field. Yet within these complexities lie answers concerning much of the deformation history that the rocks have been through. Deformation partitioning is particularly difficult to model in analogue or computer based experiments because of the immense range of heterogeneities that it involves. Such modelling has been rarely attempted, yet can reveal characteristics of the behaviour of rock during deformation that are not intuitive (e.g., Fay et al., 2009, 2008) but have been quantitatively observed (Hickey and Bell, 1999). Because of the heterogeneity of deformation partitioning in naturally deformed rocks across or along any single orogen, there is the potential that portions of rock can be found where relics of the orientation of earlier formed structures are preserved at some scale.

A consistent succession of several FIAs (foliation inflection/intersection axes preserved within porphyroblasts) across a region suggests that the porphyroblasts have not rotated (e.g., Aerden, 2004; Sayab, 2005; Ali, 2010). Dating monazite grains amongst the inclusion trails defining each FIA allows this to be tested; they should get progressively younger (e.g., Bell and Welch, 2002; Ali, 2010; Sanislav, 2010). Each phase of porphyroblast growth in such rocks appears to occur early during the crenulation deformation of a schistosity (Bell and Bruce, 2007). The entrapped FIA will have the same orientation as synchronously developing crenulation hinges or fold axes involving the same foliations in that exact location. Crenulation hinges and fold axes may change in orientation as the

* Corresponding author. Tel.: +61 747814766; fax: +61 747251501.
E-mail addresses: tim.bell@jcu.edu.au (T.H. Bell), ioan.sanislav@jcu.edu.au (I.V. Sanislav).

0191-8141/$ – see front matter © 2011 Elsevier Ltd. All rights reserved.
doi:10.1016/j.jsg.2011.03.014

deformation continues in the matrix relative to those in a porphyroblast (Bell and Bruce, 2006). However, rotation of fold axial planes during younger deformations will not affect the orientation information preserved within the porphyroblasts if the latter can be demonstrated to have not rotated.

This paper uses a dated succession of FIA trends, from a small area that contains the Swift River in western Maine where multiple phases of garnet and staurolite growth (Sanislav and Bell, 2011) occurred episodically over a 70 million year period (Sanislav, 2010), to show that they concur with a succession of overprinting of large-scale folds that dominate regional scale maps in plan view. This same relationship occurs in other orogens where similar work has been done and provides an innovative approach to deriving and integrating structural/metamorphic and pluton emplacement histories across large-scale regions.

2. Geological setting

The Central Maine Belt, a major regional unit (Fig. 1a), is bordered to the NW by NeoProterozoic basement rocks of the Bronson Hill Belt. To the SE, there is a transition from the Central Maine Belt through the Norumbega Shear Zone into the Avalon Composite Terrane. The Central Maine Belt is composed of a succession of Siluro-Devonian turbidites that form the Rangeley

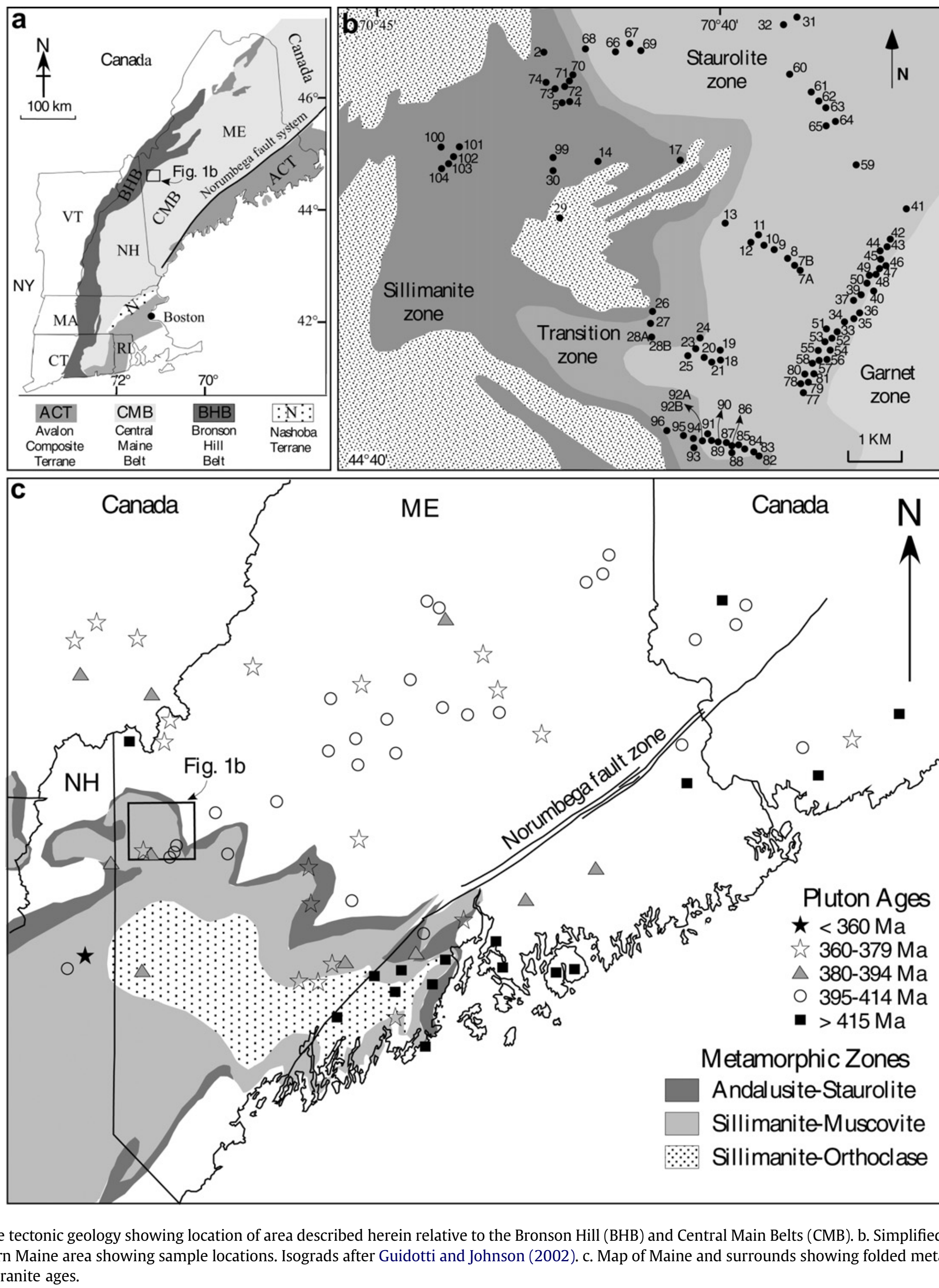

Fig. 1. a. Coarse scale tectonic geology showing location of area described herein relative to the Bronson Hill (BHB) and Central Main Belts (CMB). b. Simplified geological map of the Swift River in western Maine area showing sample locations. Isograds after Guidotti and Johnson (2002). c. Map of Maine and surrounds showing folded metamorphic isograds and the distribution of granite ages.

Stratigraphic Sequence. It was metamorphosed and deformed during the Acadian orogeny (Bradley et al., 1998) at low pressures and high temperatures with partial melting at higher grades forming migmatites (Brown and Solar, 1998a). The metamorphic grade increases from greenschist facies in the central part of the region, to upper amphibolite facies in the south (Fig. 1b and c; Guidotti, 1989). Three metamorphic events have been described. Two of them, M1 and M2, are regional scale events and the third one, M3, was regarded as pluton driven metamorphism (Holdaway et al., 1982; De Yoreo et al., 1989; Johnson et al., 2003). The area described herein (Fig. 1) contains rocks of the Rangeley and Perry Mountain Formations that were intruded by the 389–370 Ma Mooselookmeguntic pluton.

3. Fold axial planes

Methods and the resulting data lie in separate paragraphs in the following sections. Fig. 2 shows a structural geologic map of NW Maine surrounding the Swift River area in Fig. 1b (Brown and Solar, 1998a,b; Solar and Brown, 1999, 2001). Solar and Brown (1999) mapped foliations in detail across this region and constructed closely spaced form lines from their distribution. This map (Fig. 2) shows zones of complex folding separated by curvilinear belts where the foliation tends to appear more simply deformed suggesting that significant partitioning of the deformation has taken place.

The axial plane trends of all the folds visible on this map have been marked with straight lines of similar length. Their trends within a 30 km radius of the centre of the area described herein in detail are shown in the left rose plot at the base of Fig. 2; they are shown for the whole of this map in the right rose plot. The axial plane trends of all the folds visible across a large portion of the state geologic map of Maine containing this region have also been marked with straight lines of similar length in Fig. 3. Their trends across this region are plotted on the rose plot on the bottom left corner of Fig. 3.

4. Foliations in the matrix

Eighty-five spatially oriented samples were collected across the boundary between a zone of complex folding and a curvilinear belt

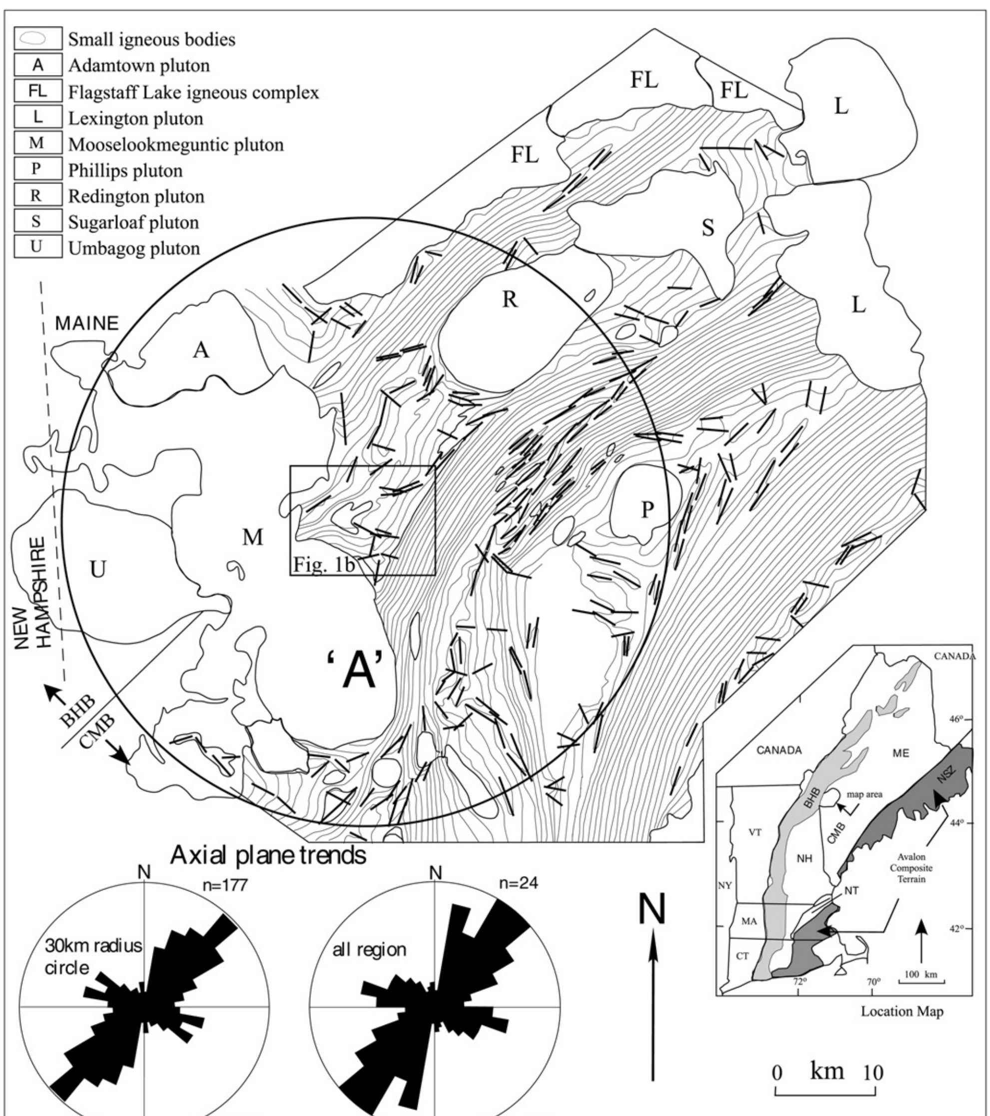

Fig. 2. Map from Solar and Brown (1999) showing their form lines for foliations. The axial planes of all folds that can be reasonably defined are marked with similar length lines. The strikes of these were measured and are shown in the accompanying rose diagrams for the 30 km circle around the Swift River area in Fig. 1b and for the whole of the map.

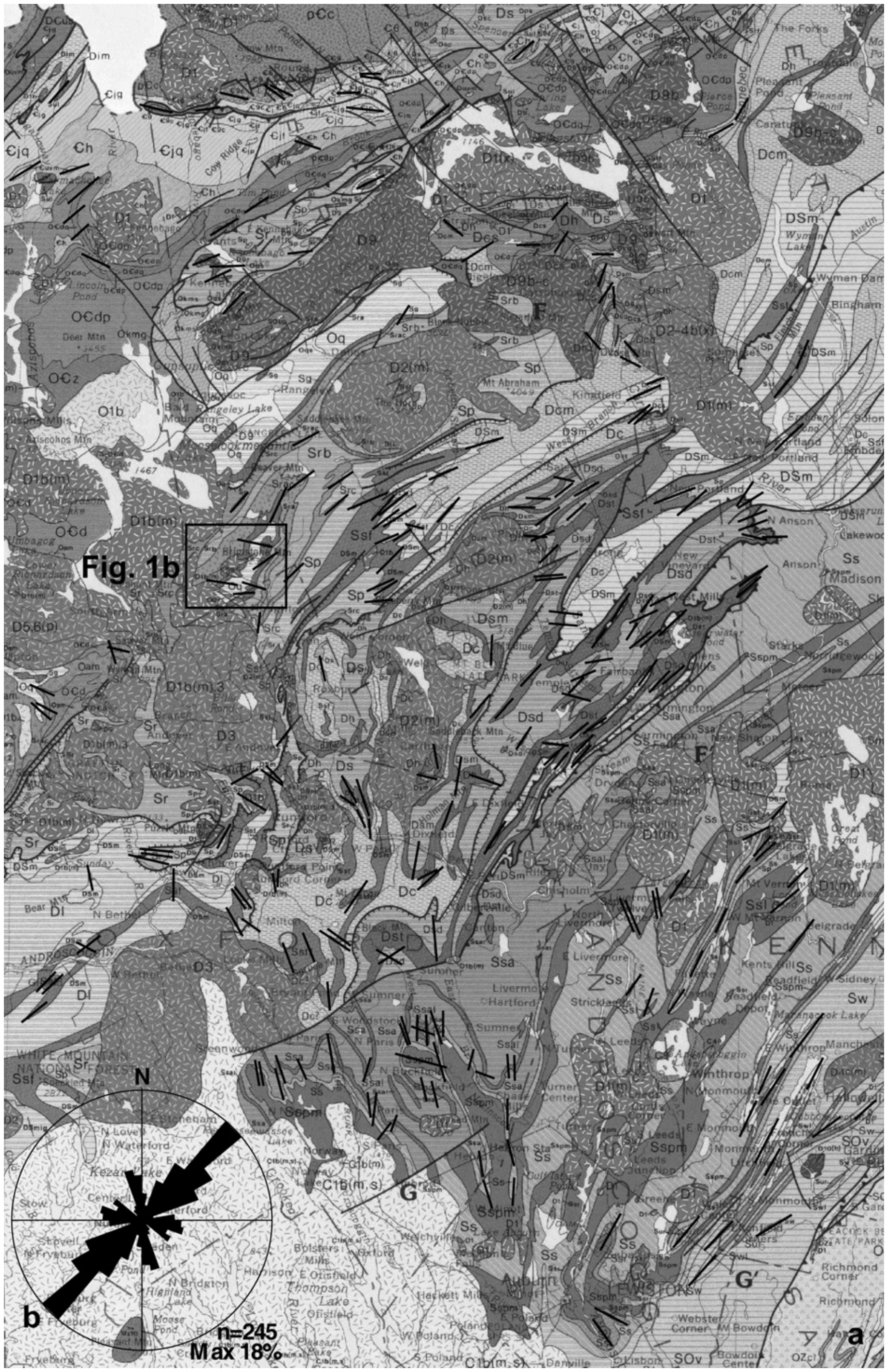

Fig. 3. a. Portion of the Maine State Survey Geological map showing the location of the Swift River area in Fig. 1b and the axial planes of all folds that can be reasonably structurally defined marked with similar length lines. b. The strikes of axial planes from (a) on a rose diagram.

close to the Mooselookmeguntic pluton (the rectangular outline labelled Fig. 1b in Fig. 2). Matrix foliations were measured in the field. They were also measured using thin sections cut after these 85 rocks were reoriented in the laboratory. For the latter measurements, horizontal rock slabs were prepared and 6 vertical thin sections 30° apart cut from them around the compass. At least 2 more vertical thin sections 10° apart were cut between some of these to measure the FIAs (see below).

The trends of the matrix foliations measured in the field and from thin sections are plotted in Fig. 4a and b respectively. The steeply ESE dipping schistosity with a pronounced NNE trend, which is characteristic of the eastern third of the area, lies within the curvilinear belt of foliation (Fig. 2) and is oriented sub-parallel to compositional layering. The more gently dipping and variably oriented foliations area to the west lie within the complexly folded domains (e.g., Solar and Brown, 2001).

5. Foliations in porphyroblasts

Foliations defined by inclusion trails in garnet and most staurolite porphyroblasts are straight except where they curve near the rim or are slightly sigmoidal with some continuous but many

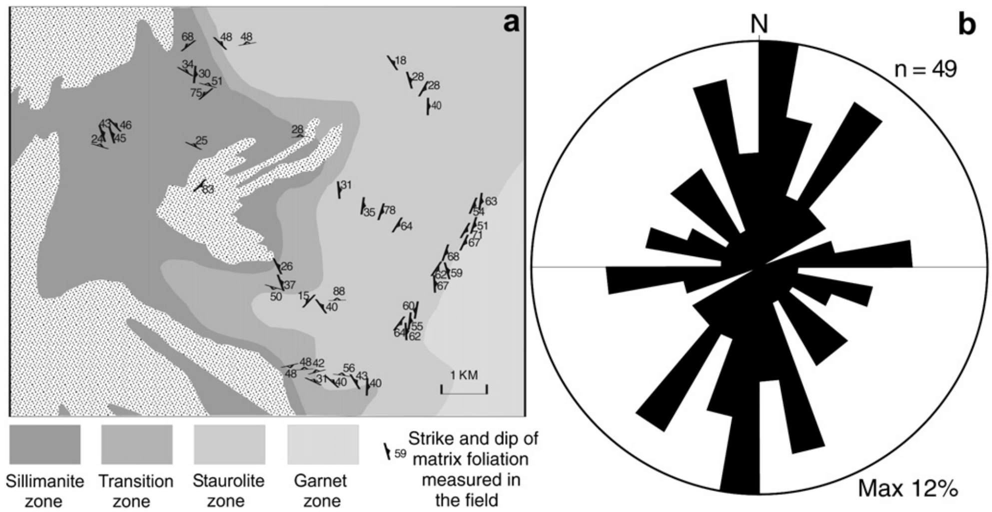

Fig. 4. a. Matrix foliations from field data plotted on map of the Swift River area shown in Fig. 1b. b. The strikes of matrix foliations measured from at least 8 thin sections per sample plotted on a rose diagram.

truncated by the matrix foliation (Fig. 5a–c). Some in staurolite define a differentiated crenulation cleavage (Fig. 5d and e) at stage 3 or 4 (e.g., Ham and Bell, 2004). Andalusite is present in a few samples as big poikilitic porphyroblasts that have overgrown the matrix foliation. Cordierite is commonly at least partly replaced by biotite or muscovite grains that are larger than those in the matrix and aligned with the matrix foliation. The apparent dips of foliations preserved as inclusion trails in staurolite porphyroblasts were measured from the same thin sections used to measure the matrix foliation. As shown in Fig. 5f, these pitches were measured from the centre of porphyroblasts and from their rims where a truncational foliation was present. Following the procedure described above, 30–140 pitches per sample were measured from at least eight vertically oriented thin sections with different strikes, yielding a total of 2010 measurements for garnet and 2350 for staurolite. The results were plotted on stereographic projections (shown for staurolite only in Fig. 6a) with the program GEOrient v.9.4.0 of Rod Holcombe (http://www.holcombe.net.au/software) for each sample and microstructural domain (core, median or rim-inclusion trails), so that the strike and dip for the foliations preserved in garnet and staurolite porphyroblasts could be determined.

The strikes of the inclusion trail foliations were plotted on rose diagrams from which 4 major trends can be defined for garnet (Fig. 6b; dips shown in Fig. 6c) and 5 for staurolite (Fig. 6d; dips shown in Fig. 6e). Comparing Fig. 6b and d, 4 of the peaks in garnet foliation trends correlate with those in staurolite with most foliations striking WSW–ENE and ~N–S in garnet and SW–NE and WNW–ESE in staurolite. The dips of these foliations in both porphyroblastic phases are predominantly sub-vertical (Fig. 6c and e) whereas in the matrix they spread around 45° (Fig. 6f).

6. FIAs

FIAs in both garnet and staurolite porphyroblasts were measured using the minimum of 8 thin sections per sample mentioned above, by locating the two 30° apart between which the inclusion trail asymmetry changed and then refining this to within 10° by cutting 2 more (Hayward, 1990; Bell and Hickey, 1999). These thin sections are the same as those from which the foliations defined by inclusion trails within porphyroblasts mentioned above were measured. A total of 75 FIAs for garnet porphyroblasts (Fig. 6g) and 76 for staurolite (Fig. 6h) were measured.

These FIA data are shown in Table 1. Five peaks occur in the combined distribution of garnet and staurolite FIAs (Fig. 7a). Core to rim changes in FIA trend were found in staurolite porphyroblasts for 16 samples as shown in Fig. 7b. Staurolite porphyroblast cores with WNW–ESE trending FIAs are succeeded by N–S, W–E and WSW–ENE rims. N–S trending FIA cores and pre-FIAs are succeeded by SW–NE rims. W–E trending FIAs cores are succeeded by WSW–ENE medians/rims and SW–NE rims. WSW–ENE trending cores are succeeded by SW–NE trending rims.

7. Interpretation

7.1. FIA succession

At least two deformation events are needed to define a FIA with the first having to be sufficiently intense to form a foliation. Porphyroblast growth at the start of the second deformation traps the previously formed foliation within it (e.g., Bell et al., 2003). The effects of the latter event are most commonly preserved as curvature of the pre-existing foliation just inside the rim of a porphyroblast independent of how intense the newly developing foliation becomes in the matrix; sigmoidally curved inclusion trails are much less common. The axis of curvature, which equates with the intersection between the first foliation and the axial plane of the second event, which may or may not develop further into a foliation, determines the FIA trend. A FIA trend obtained from the core of a porphyroblast must be older than a differently trending FIA from the rim (e.g., Ham and Bell, 2004).

In western Maine, sixteen samples contain staurolite porphyroblasts where the trend of the FIA changes from the core to the rim. These data indicate that the 5 peaks in the FIA distribution shown in Fig. 7a resulted from a succession of FIA trends that is consistent for all samples containing more than one FIA (Fig. 7b). This succession has been independently confirmed by dating (Fig. 8a; Sanislav and Shah, 2010; Sanislav, 2010) and starts with a FIA trending WNW–ESE (FIA 1 not dated), shifts to N–S (FIA 2, 408 ± 10 Ma), W–E (FIA 3, 388 ± 9 Ma), WSW–ENE (FIA 4, 372 ± 5 Ma) and finally SW–NE (FIA 5, 353 ± 4 Ma). Although the WNW–ESE trending FIA 1 has not been dated, it coincides with the

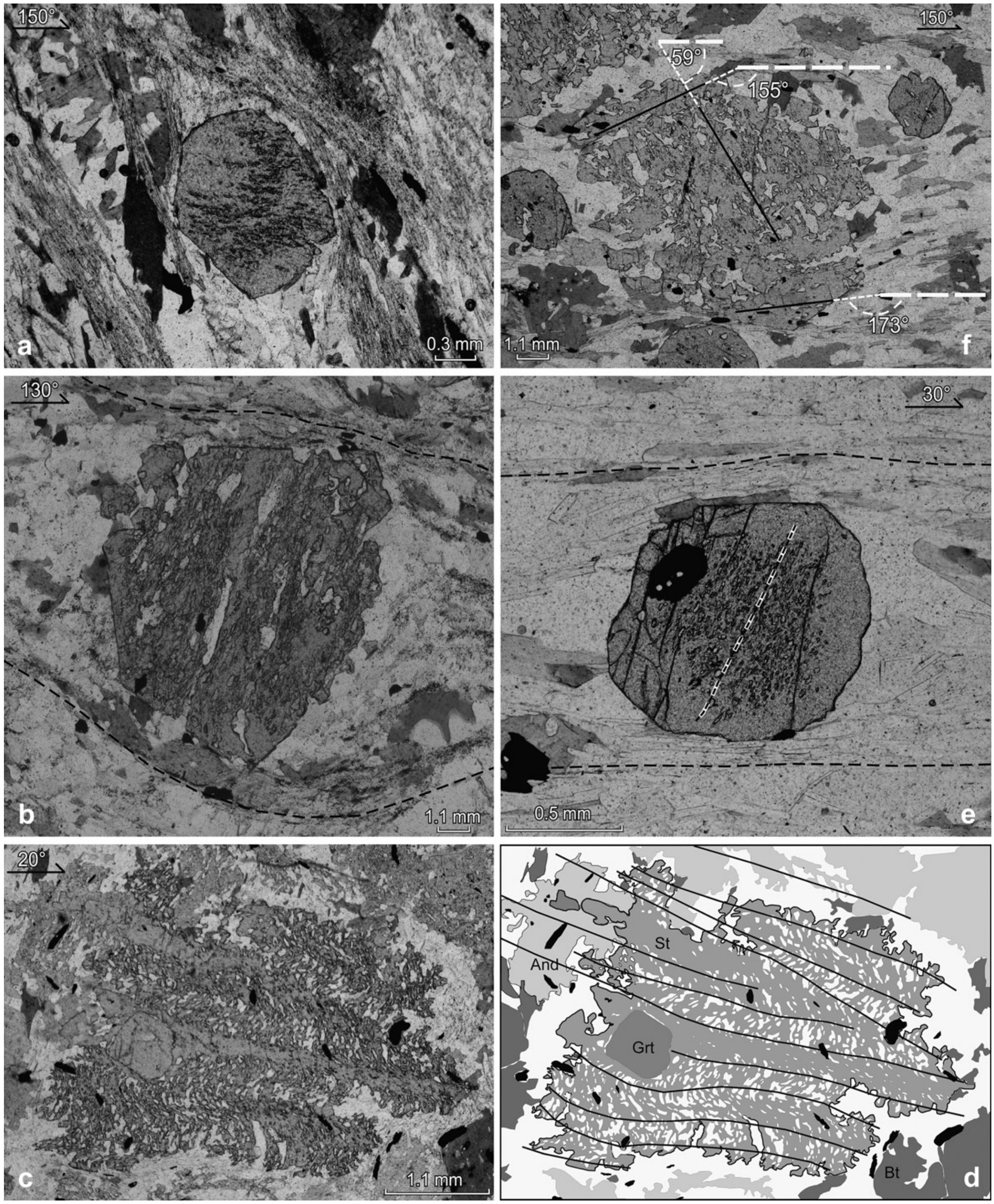

Fig. 5. a. Photomicrograph showing the relationship between inclusion trails in a garnet porphyroblast and the matrix foliation. The few samples containing garnet porphyroblasts that overgrew a sub-horizontal fabric are truncated by the matrix foliation. Plane polarized light. Vertical thin section. Single barbed arrow indicates strike and way up. Sample IS37. b. Photo of a staurolite porphyroblast with steeply pitching inclusion trails truncated by the gently pitching matrix foliation. Plane polarized light. Vertical thin section. Single barbed arrow indicates strike and way up. Sample IS90. c,d. Photo and line diagram of a staurolite porphyroblast that preserves a differentiated crenulation cleavage (stage 4) as inclusion trails. Andalusite locally has replaced the staurolite rim. Plane polarized light. Vertical thin section. Single barbed arrow indicates strike and way up. Sample IS73. e. Photo of a garnet porphyroblast with steeply pitching inclusion trails truncated by the sub-horizontally pitching matrix foliation. Plane polarized light. Vertical thin section. Single barbed arrow indicates strike and way up. Sample IS12. f. Photo showing how measurements were made of the pitch of foliations in vertical thin sections defined by inclusion trails in the core and rim of a staurolite porphyroblast. The rim-inclusion trails appear to be continuous with those in the matrix. Plane polarized light. Vertical thin section. Single barbed arrow indicates strike and way up. Sample IS17.

form surface for the FIA 1 generated garnet, staurolite, andalusite and sillimanite isograds across Maine and the distribution of >420 Ma aged plutons (Fig. 1c; Bradley et al., 1998) and appears to have formed around 420 Ma.

7.2. Steeply vs gently dipping foliations and FIAs

Where a steep foliation is overprinted by a deformation with a gently dipping axial plane, or a gently dipping foliation is

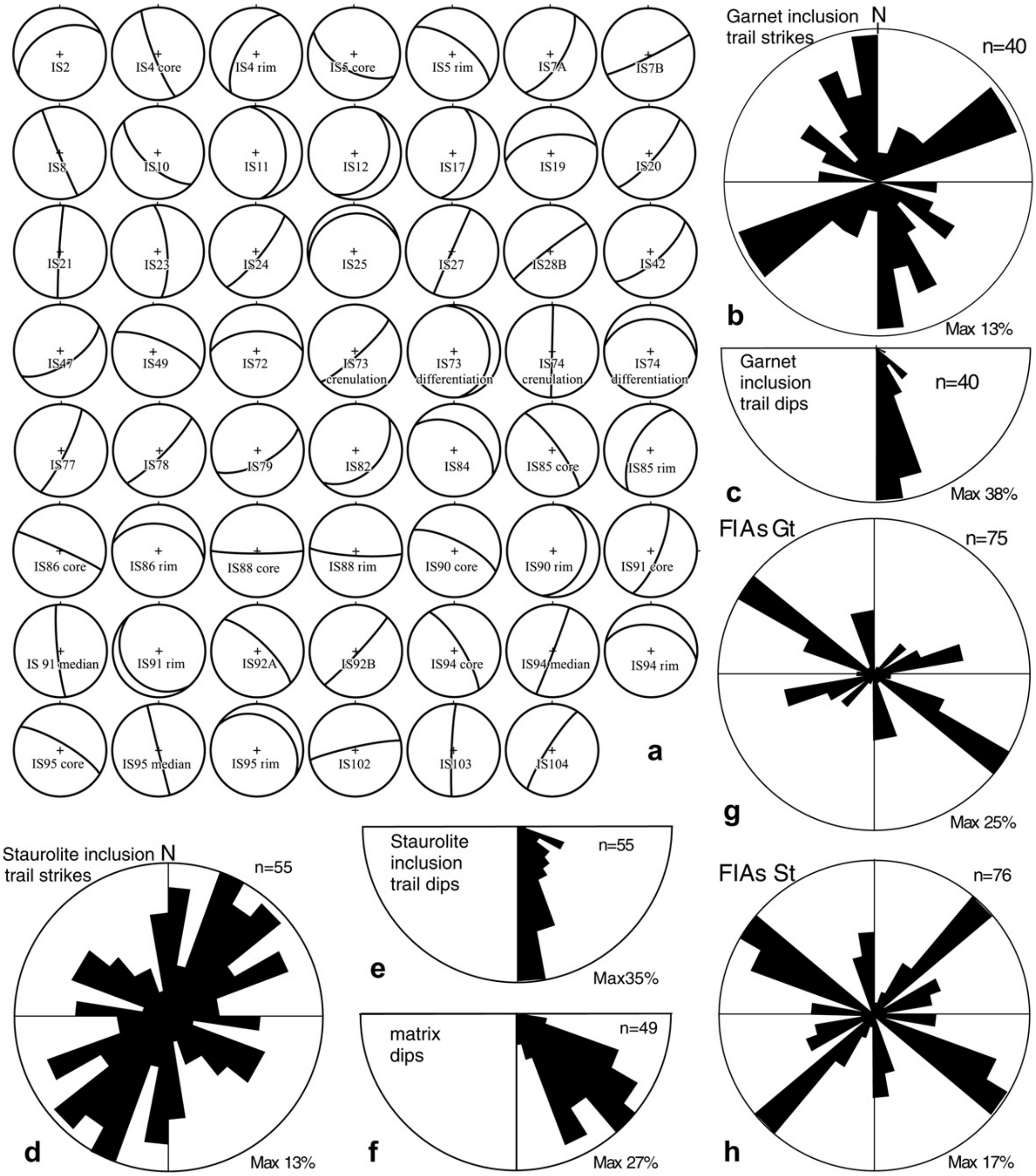

Fig. 6. a. Foliations plotted on stereo nets calculated from inclusion trail pitches measured from a minimum of 8 thin sections per each sample indicated. b–e. Equal-area rose diagrams of the trends (b,d) and the dips (c,e) of the foliations measured from the stereo nets for staurolite shown in (a) and garnet porphyroblasts (not shown). Also shown are rose diagrams for (f) the dip of the matrix foliation measured in the samples from (a) and the FIAs for garnet (g) and staurolite (h).

overprinted by a deformation with a steeply dipping axial plane, the trend of the FIA is controlled by the steep structures (e.g., Fig. 8b). That is, very steep foliations preserved in garnet and staurolite should have similar trends to the FIAs measured from those porphyroblasts as shown in Fig. 8b. Fig. 6c and e shows that most foliations preserved in garnet and staurolite porphyroblasts are steeply dipping, mainly ranging from 60° to 90°. Fig. 9a–c compares the strikes of all foliations preserved as inclusion trails within garnet and staurolite porphyroblasts and the matrix respectively, with the FIA trends for garnet, staurolite or both phases combined (Fig. 9d–f, respectively). It shows that the strikes of foliations preserved inside the porphyroblasts correlate well with the FIA trends suggesting that most are steeply dipping, as is supported by Fig. 6c and e. The strike of foliation in the matrix (Fig. 9c), which was measured for each sample using the same thin sections, does not correlate as clearly with the FIA trends (Fig. 9f), which is no surprise since these foliations have moderate dips (Fig. 6f) due to the folding effects of the various deformations that each was subjected to after the porphyroblasts formed including those of reactivation (e.g., Ham and Bell, 2004).

7.3. FIAs vs fold axial planes

Deformation during orogenesis forms folds and foliations with the latter forming sub-parallel to axial planes of the former. The trends of the axial planes of folds observable on regional maps are

Table 1
List of FIA measurements for garnet and staurolite porphyroblasts. c – core-inclusion trails; m – median-inclusion trails; r – rim-inclusion trails; p – pre-FIA.

Sample no.	FIA 1		FIA 2		FIA 3		FIA 4		FIA 5	
	St	Grt	St	Grt	St	Grt	St	Grt	St	Grt
IS2		125					75			
IS4	125	125	165r							
IS5	125c	120			95r					
IS7a	125	115								
IS7b									15	40
IS8									45	45
IS9b		120					65			
IS10		115							30	
IS11		120							35	
IS12				145					35	
IS13		125								
IS14		120							40	
IS17	125	125					75			
IS18			165	165						
IS19				165	95					
IS20			165	165						
IS21			175	175						
IS23					95	95				
IS24								75	45	
IS25		120							45	
IS26								75		
IS27							75	75		
IS28a										35
IS28b		130							25	
IS29		115								
IS30	120	115								
IS33								65		
IS34								85		
IS35		125								
IS36								75		
IS37								65		
IS42	115	125								
IS43	110	125								
IS45								75		
IS46				175						
IS47	115	125								
IS49	110	125								
IS50				175						
IS52	110	125								
IS53								75		
IS54	115	115								
IS55			175	175						
IS56			175c	175					45r	
IS57	120	110								
IS59				165						
IS60								75		
IS61								75		
IS62				160						
IS63				160						
IS64				170						
IS65								75		
IS66	125	125								
IS67								65	40	
IS68	125	115								
IS69								65		
IS70										25
IS71									40	45
IS72				175			65			
IS73			165p	165					45	
IS74							75p	75	40	
IS77			170c	170					45r	
IS78									55	
IS79	110									
IS81										45
IS82							65			
IS83	120	110								
IS84	125									
IS85							65c	65	35r	
IS86	115c						75r			
IS87	115									
IS88					90c				95r	
IS89	115	115								
IS90	130c	120	165r							
IS91					100c		85m		45r	
IS92a			170							
IS92b	125									
IS93			165	165						
IS94					90c	100	65m		25r	
IS95					95c	95	65m		35r	
IS96								65		
IS99								70		
IS101				155						
IS102									45	45
IS103	120	125								

dominated by those with steeply rather than gently dipping axial planes because:-

1. those with horizontal axial planes are not recorded unless there is extreme topographic variation,
2. heterogeneous strain plus topographic variation spreads the trend of those with gently dipping axial planes around the compass,
3. newly forming folds with steeply dipping axial planes tend to rotate any gently dipping axial planes of previously formed folds towards their own axial plane trend.

If deformation partitions on all scales in every event, portions of even the very first formed folds could be preserved un-rotated by the effects of younger deformation events. This possibility is supported by the fact that measurement of FIAs around large-scale regional folds commonly reveals that they were the first folds to form (e.g., Bell et al., 2003; Ham and Bell, 2004; Bell and Newman, 2006). They probably survive because thick sedimentary packages are least disturbed prior to the onset of folding and develop with the largest wavelengths and amplitudes (Hobbs et al., 1976). Gravitational collapse and spreading locally rotates their axial planes to shallow dips, resulting in smaller wavelengths for subsequently formed folds with upright axial planes; cyclic repetition of this process would reduce fold wavelength with time (e.g., Talbot, 1987). Therefore, within the distribution of the axial plane strikes obtained from maps of folds across the region shown in Figs. 2 and 3, relics should be preserved of the trends of the folds in the orientation in which they formed. Fig. 9g–i reproduces the rose plots constructed from the regional distribution of axial plane trends in Figs. 2 and 3 so that they can be directly compared with FIA trends in Fig. 9f. The 5 trend lines chosen to best reflect the distribution of FIA trends in Fig. 9f lie on or within 10° of a peak in the regional distribution of fold axial planes in each case, with the exception of FIA 4. However, the 20° spread of data for FIA 4 overlaps with the broad peak that tends to surround FIA 5 in the axial plane trends. Consequently, the distribution of fold axial plane trends in this portion of Maine at a regional scale on a rose diagram preserves the orientation of each generation of folds with steeply dipping axial planes that accompanied porphyroblast growth and controlled FIA development. Fig. 9i shows that an extra peak appears on the rose diagram when the axial planes of all the folds visible in Fig. 2 are used rather than just those within a 30 km radius of area shown in Fig. 1b. This may indicate that a period of bulk shortening partitioned into the east that did not affect the rocks to the west. Such a phenomenon has been recognized elsewhere at a range of scales (Spiess and Bell, 1996; Bell and Mares, 1999; Bell et al., 2004; Yeh and Bell, 2004). Alternatively, foliation development at this time was not accompanied by porphyroblast

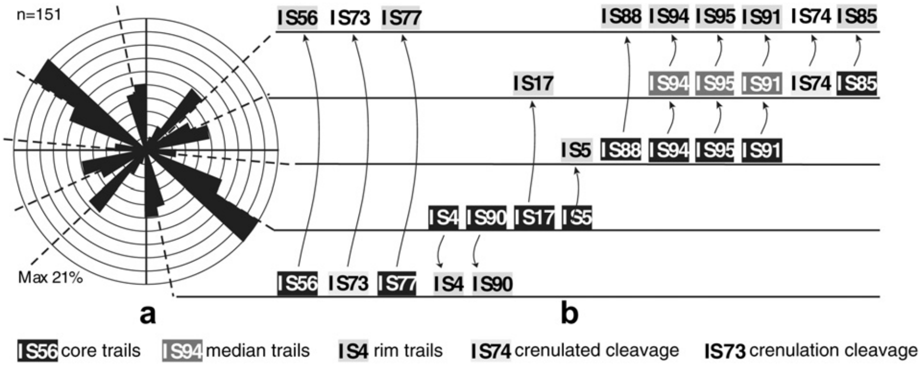

Fig. 7. Equal-area rose diagram for all FIAs showing how the relative FIA succession was established. Arrows show core to rim changes in staurolite porphyroblasts. The total combinations of changes reveal a succession that is consistent between the samples.

growth because there is a similar peak within the trends of foliations in the schistose matrix of porphyroblast bearing samples (compare Fig. 9c and i).

8. Discussion

8.1. Fold axial planes, FIAs and structural successions in multiply deformed rocks

At pressures of 2.5 kb or more, folds in previously cleaved rocks are commonly accompanied by the development of crenulation hinges in pelites. For appropriate bulk compositions and temperatures, early during the development of such crenulations, porphyroblasts grow over the foliation being crenulated within the crenulation hinge (e.g., Bell and Bruce, 2006, 2007). Where the foliation being crenulated is gently dipping and regional folds with steeply dipping axial planes form, the intersection of the steeply dipping axial plane with the gently dipping foliation is preserved as an inflection of the latter in the rim of the porphyroblast. If folding intensifies and a new steeply dipping matrix foliation forms against the rim of the porphyroblast, then this may become entrapped by a successive phase of porphyroblast growth in a subsequent deformation event and preserve an intersection lineation between the 2 foliations rather than just an inflection. These structures are the FIAs. Where a steeply dipping axial plane foliation of regional folds is being crenulated and crenulations develop with gently dipping axial planes, a similar relationship develops (Bell and Bruce, 2006). In both situations, FIAs directly reflect the strikes of the fold axial planes that are steeply dipping. Significantly, quantitative measurement of the inclusion trails in porphyroblasts in vertical thin sections has revealed that most are steeply or gently pitching rather than having intermediate pitches (e.g., Fig. 6c and e plus fig. 10 in Hayward, 1992 and figs. 10 and 12 in Bell and Newman, 2006). Therefore, it should be no surprise that the trends of the axial planes of regional folds plotted on a rose diagram reflect the distribution of FIAs. The fact that the 5 trend lines chosen to best reflect the distribution of FIA trends in Fig. 9f lie on or within 10° of a peak in the regional distribution of fold axial planes in each case, with the exception of FIA 4, indicates the following possibility. It suggests that the range of orientations in which the various generations of folds actually formed can be assessed simply by marking all axial planes of folds on a regional map, and plotting rose diagram of their trends. It also suggests that peaks in fold trends on a rose diagram provide a rapid first pass to determining the number of FIAs present in a region and a direct indication of the number of significant changes in direction of bulk shortening, and thus relative plate motion, that accompanied orogenesis. Indeed, the fold axial plane data from across the whole of the region shown in Fig. 2 suggest that an extra SSW–NNE trending FIA set could be found in rocks to the east of the area described in detail herein (Fig. 9i).

8.2. Timing fold generations

Superficially the belts of curvilinear foliation trend surfaces in Fig. 2 look younger than the complex folded zones that lie between them. However, they vary in orientation from N–S adjacent to

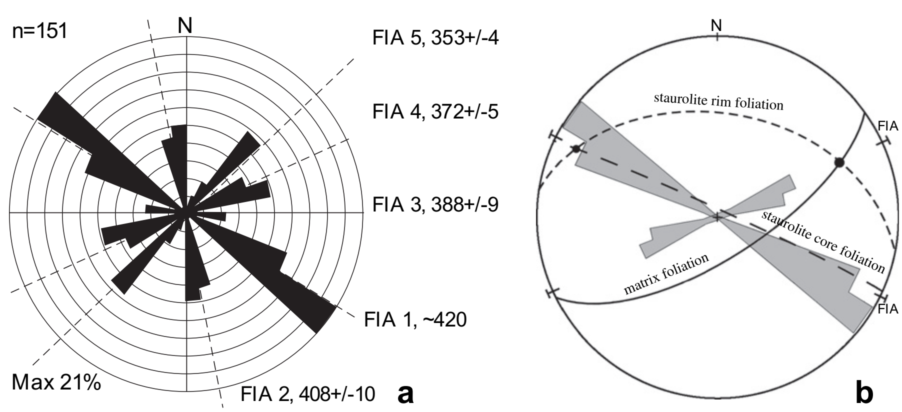

Fig. 8. a. Shows the FIA succession and the ages in million years obtained by Sanislav (2010) for 4 of the FIA sets. The first was estimated using granite ages along the same trend from Fig. 1c. b. Shows the relationships between FIAs 1 and 4 (the shaded areas) measured by the asymmetry method in staurolite porphyroblasts for all samples (from Fig. 6g), and the foliations measured from inclusion trails within staurolite porphyroblasts as well as the matrix foliation in Sample IS86 (from Fig. 6a). The T-shapes on the edge of the stereo net mark the trend of the intersection axes between the core and rim as well as the rim and matrix foliations and coincide with the measured FIA trends.

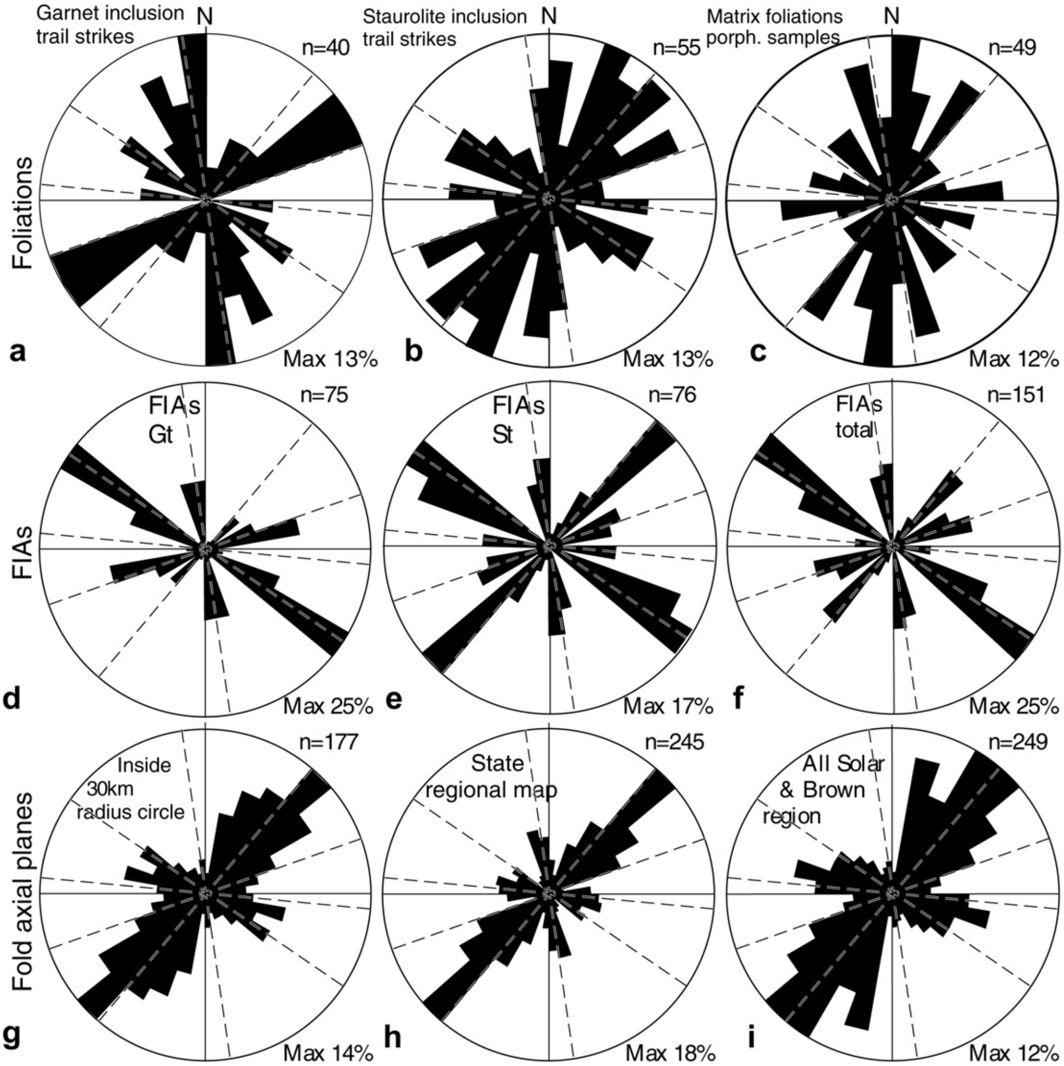

Fig. 9. Rose diagrams comparing foliations measured from garnet (a) and staurolite (b) porphyroblasts, the matrix of those samples (c) FIAs measured from garnet (d) and staurolite (e) and all porphyroblasts (f), and the trends of fold axial planes measured from the 30 km radius circle around the area studied in detail in Fig. 2 (g), the State regional map in Fig. 3 (h) and the whole of the region in Fig. 2 (i).

location 'A' where they are cut by the Mooselookmeguntic pluton, to WSW–ENE. To the east of location 'A', NW–SE trend fold axial planes are present that are not obvious where the curvilinear foliation trend surfaces trend more SW–NE. This suggests that the N–S trending portions were rotated to WSW–ENE trends after the NW–SE trending folds formed and this rotated or destroyed these folds because the latter folds formed at an earlier time. Folds trending SW–NE and W–E are present both east of location 'A' and in the SW–NE trending portions of the curvilinear foliation trend surfaces suggesting they formed after the N–S trending portion adjacent to location 'A'. Thus a crude timing succession of NW–SE, N–S, and then one of W–E or SW–NE folding events occurred. This can be compared with the FIA succession where the relative timing has been quantitatively ascertained (Fig. 7a) and checked independently by dating (Fig. 8; Sanislav, 2010). It is supported by the Mooselookmeguntic pluton forming between 389 and 370 Ma, after the N–S trending FIA 2 formed at 408 ± 10 Ma.

8.3. Dating FIA successions

A FIA results from a succession of foliations that form over a period of time while the direction of horizontal bulk shortening, which presumably relates to a period of constant relative plate motion (e.g., Bell and Newman, 2006), remains constant. The relative plate motion between Africa and Europe changed 8 times in 115 million years suggesting changes every 15 million years on average (Platt et al., 1989). It is important to realize that the succession of FIAs (Fig. 7) and ages shown in Fig. 8 does not indicate that deformation was restricted to one point in time for each FIA. Each FIA requires at least 1 foliation and 1 subsequent deformation to form. In general each results from the overprinting of three or more deformations with 7 being common in Vermont (e.g., Bell et al., 2003; Bell and Newman, 2006). Foliations cannot be correlated with certainty from sample to sample. However, as shown in Fig. 7, consistent successions of FIAs can be quantitatively distinguished, allowing data obtained from different samples with the same FIA to be combined. Sanislav (2010) obtained each date shown in Fig. 8 by selecting two samples containing just one of the 5 FIA trends preserved within porphyroblasts and searching for monazite grains within the foliations defined by the inclusion trails. The foliations containing these monazite grains formed somewhere within a 5–25 million year time frame during which the direction of horizontal bulk shortening did not change and several foliation forming events occurred about the one FIA trend. Consequently, averaging the ages of monazite grains within inclusion trails from two samples containing the same FIA trend provides a date that will lie somewhere within the 5–25 million year period of time over which the successive foliations defining that FIA trend formed. However, the date obtained could be at the start, half way through or at the end of that time frame and thus be close to or a long way from that obtained for the previous or subsequently formed FIA. Dating more samples reduces any overlap in the errors from one FIA trend age to the next but the potential for multiple foliation development and any associated fold effects (e.g., Bell and Hickey, 1998) throughout that period of time must be kept in mind.

8.4. Encapsulation of the bulk of fold belt orogenic history within a small area

The samples described herein were obtained from <50 km^2 of the area shown in Fig. 1b and outlined in Figs. 1c, 2 and 3. Yet they preserve the episodically continuous effects of a lengthy history spanning ~70 million years of deformation and metamorphism (Figs. 5–8) that affected more than the 25,000 km^2 covered by the regional map in Fig. 3. Furthermore, this history spans ~65 million years of pluton emplacement that affected the large-scale region shown in Fig. 1c (Sanislav and Bell, 2011). For example, the isograd form surface in Fig. 1c developed parallel to the trend of FIA 1 around the first period of pluton emplacement at 420 Ma (Fig. 8a; Sanislav and Bell, 2011). Similar relationships between FIA ages and the regional timing of pluton emplacement have been revealed in other regions (e.g., Cao, 2009) where fold axial planes are distributed relative to FIAs in a similar manner to that described herein (Cao, 2010; Shah, 2010). Such encapsulation of the large-scale regional tectonic history by porphyroblasts within a small area in several orogens suggests FIAs provide a powerful tool for quickly accessing the tectonic history over an extended period of orogeny within a region. This appears to result from the fact that porphyroblast growth becomes significant during regional metamorphism at around 520–540 °C (e.g., Evans, 2004; Shah, 2009; Sanislav and Bell, 2011). This heat, plus the contrast in competency with the rock matrix that porphyroblasts provide, appears to result in most deformations, and the effects of metamorphism that accompanies each event, being partitioned to some degree through this location.

Acknowledgements

We acknowledge the ARC and James Cook University for research and scholarship funds. We further acknowledge James Cook University for the excellent facilities that they have made available for conducting this type of research. We thank the referees, Gary Solar and Chris Talbot, for their constructive comments.

References

Aerden, D.G.A.M., 2004. Correlating deformation in Variscan NW Iberia using porphyroblasts; implications for the Ibero-Armorican Arc. Journal of Structural Geology 26, 177–196.

Ali, A., 2010. The tectono-metamorphic evolution of the Balcooma Metamorphic Group, north-eastern Australia: a multidisciplinary approach. Journal of Metamorphic Geology 28, 397–422.

Bell, T.H., 1983. Thrusting and duplex formation at Mount Isa, Queensland, Australia. Nature 304, 493–497.

Bell, T.H., 1991. The role of thrusting in the structural development of Mt Isa Mine and its implications for exploration in the surrounding region. Economic Geology 86, 1602–1625.

Bell, T.H., Bruce, M.D., 2006. The internal inclusion trail geometries within a first phase of porphyroblast growth. Journal of Structural Geology 28, 236–252.

Bell, T.H., Bruce, M.D., 2007. Progressive deformation partitioning and deformation history: evidence from millipede structures. Journal of Structural Geology 29, 18–35.

Bell, T.H., Hickey, K.A., 1998. Multiple deformations with successive sub-vertical and sub-horizontal axial planes: their impact on geometric development and significance for mineralization and exploration in the Mount Isa region. Economic Geology 93, 1369–1389.

Bell, T.H., Hickey, K.A., 1999. Complex microstructures preserved in rocks with a simple matrix: significance for deformation and metamorphic processes. Journal of Metamorphic Geology 17, 521–536.

Bell, T.H., Mares, V.M., 1999. Correlating deformation and metamorphism around arcs in orogens. The American Mineralogist 84, 1727–1740.

Bell, T.H., Newman, R., 2006. Appalachian orogenesis: the role of repeated gravitational collapse. In: Butler, R., Mazzoli, S. (Eds.), Styles of Continental Compression. Special Papers of the Geological Society of America, vol. 414, pp. 95–118.

Bell, T.H., Welch, P.W., 2002. Prolonged Acadian orogenesis: revelations from foliation intersection axis (FIA) controlled monazite dating of foliations in porphyroblasts and matrix. American Journal of Science 302, 549–581.

Bell, T.H., Ham, A.P., Hickey, K.A., 2003. Early formed regional antiforms and synforms that fold younger matrix schistosities: their effect on sites of mineral growth. Tectonophysics 367, 253–278.

Bell, T.H., Ham, A.P., Kim, H.S., 2004. Partitioning of deformation along an orogen and its effects on porphyroblast growth during orogenesis. Journal of Structural Geology 26, 825–845.

Bradley, D.C., Tucker, R.D., Lux, D., Harris, A.G., McGregor, D.C., 1998. Migration of the Acadian Orogen and Foreland Basin across the Northern Appalachians. U.S. Geological Survey, Open-file report, 98–770, 79 p.

Brown, M., Solar, G.S., 1998a. Shear zone systems and melts: feedback relations and self organization in orogenic belts. Journal of Structural Geology 20, 211–227.

Brown, M., Solar, G.S., 1998b. Granite ascent and emplacement during contractional deformation in convergent orogens. Journal of Structural Geology 20, 1365–1393.

Cao, H., 2009. Chemical U-Th-Pb monazite dating of deformations versus pluton emplacement and the proterozoic history of the Arkansas River region, Colorado, USA. Acta Geologica Sinica 83, 917–926.

Cao, H., 2010. Multiple successions of foliation development in shallow versus deep orogenic regimes and their relationship to regional folding. In: 10th International Multidisciplinary Scientific Geoconference (SGEM), vol. 1, pp. 121–128.

De Yoreo, J.J., Lux, D.R., Guidotti, C.V., Decker, E.R., Osberg, P.H., 1989. The Acadian thermal history of western Maine. Journal of Metamorphic Geology 7, 169–190.

Evans, T.P., 2004. A method for calculating effective bulk composition modification due to crystal fractionation in garnet-bearing schist: implications for isopleth thermobarometry. Journal of Metamorphic Geology 22, 547–557.

Fay, C., Bell, T.H., Hobbs, B.E., 2008. Porphyroblast rotation versus non rotation: conflict resolution! Geology 36, 307–310.

Fay, C., Bell, T.H., Hobbs, B.E., 2009. Porphyroblast rotation versus nonrotation: conflict resolution! Reply. Geology 37, e188.

Guidotti, C.V., 1989. Metamorphism in Maine: an overview. In: Studies in Maine Geology, vol. 3, pp. 1–19.

Guidotti, C.V., Johnson, S.E., 2002. Pseudomorphs and associated microstructures of western Maine, USA. Journal of Structural Geology 24, 1139–1156.

Ham, A.P., Bell, T.H., 2004. Recycling of foliations during folding. Journal of Structural Geology 26, 1989–2009.

Hayward, N., 1990. Determination of early fold axis orientations in multiply deformed rocks using porphyroblast inclusion trails. Tectonophysics 179, 353–369.

Hayward, N., 1992. Microstructural analysis of the classic snowball garnets of southeast Vermont. Evidence for non-rotation. Journal of Metamorphic Geology 10, 567–587.

Hickey, K.A., Bell, T.H., 1999. Behaviour of rigid objects during deformation and metamorphism: a test using schists from the Bolton Synform, Connecticut. Journal of Metamorphic Geology 17, 211–228.

Hobbs, B.E., Means, W.D., Williams, P.F., 1976. An Outline of Structural Geology. Wiley, NY, 571 p.

Holdaway, M.J., Guidotti, C.V., Novak, J.M., Henry, W.E., 1982. Polymetamorphism in medium- to high-grade pelitic metamorphic rocks, west-central Maine. Geological Society of America Bulletin 93, 572–584.

Johnson, T.E., Brown, M., Solar, G.S., 2003. Low-pressure subsolidus and suprasolidus phase equilibria in the MnNCKF-MASH system: constraints on conditions of regional metamorphism in western Maine, northern Appalachians. American Mineralogist 88, 624–638.

Loosveld, R.J.H., 1989. The synchronism of crustal thickening and high T/low P metamorphism in the Mount Isa Inlier, NW Queensland, Australia. Part 1. An example, the central Soldiers Cap Group. Tectonophysics 158, 173–190.

Loosveld, R.J.H., Etheridge, M.A., 1990. A model for low-pressure facies metamorphism during crustal thickening. Journal of Metamorphic Geology 8, 257–267.

Passchier, C.W., Kroner, A., Myers, J.S., 1990. Field Geology of High-grade Gneiss Terrains. Springer-Verlag, Berlin. 251 p.

Platt, J.P., Behrmann, J.H., Cunningham, P.C., Dewey, J.F., Helman, M., Parish, M., Shepley, M.G., Wallis, S., Weston, P.J., 1989. Kinematics of the Alpine arc and the motion history of Adria. Nature 337, 158–161.

Sanislav, I.V., 2010. A long lived metamorphic history in the contact aureole of the Mooselookmeguntic pluton revealed by in-situ dating of monazite grains preserved as inclusions in staurolite porphyroblasts. Journal of Metamorphic Geology 29, 251–273.

Sanislav, I.V., Bell, T.H., 2011. The inter-relationships between long-lived metamorphism, pluton emplacement and changes in the direction of bulk shortening during orogenesis. Journal of Metamorphic Geology 29, in press.

Sanislav, I.V., Shah, A.A., 2010. The problem, significance and implications for metamorphism of 60 million years of multiple phases of staurolite growth. Journal of the Geological Society of India 6, 384–398.

Sayab, M., 2005. Microstructural evidence for N–S shortening in the Mount Isa Inlier, NW Queensland, Australia; the preservation of early W–E-trending foliations in porphyroblasts revealed by independent 3D measurement techniques. Journal of Structural Geology 27, 1445–1468.
Sayab, M., 2006. Decompression through clockwise P-T path: implications for an early N-S shortening orogenesis in the Mesoproterozoic Mt Isa Inlier (NE Australia). Journal of Metamorphic Geology 24, 89–105.
Shah, A.A., 2009. FIAs (foliation intersection/inflection axes) preserved in porphyroblasts, the DNA of deformation: a solution to the puzzle of deformation and metamorphism in the Colorado Rocky Mountains, USA. Acta Geologica Sinica 83, 971–984.
Shah, A.A., 2010. Tectono-metamorphic Evolution of Big Thompson Canyon Region Colorado Rocky Mountains, USA. Unpublished PhD thesis, James Cook University, 208 p.
Solar, G.S., Brown, M., 1999. The classic high-T – low-P metamorphism of west-central Maine, USA: is it post-tectonic or syn-tectonic? Evidence from porphyroblast-matrix relations. Canadian Mineralogist 37, 311–333.
Solar, G.S., Brown, M., 2001. Deformation partitioning during transpression in response to Early Devonian oblique convergence, northern Appalachian orogen, U.S.A. Journal of Structural Geology 22, 1043–1065.
Spiess, R., Bell, T.H., 1996. Microstructural controls on sites of metamorphic reaction: a case study of the inter-relationship between deformation and metamorphism. European Journal of Mineralogy 8, 165–186.
Talbot, C.J., 1987. Strains and vorticity beneath a tabular batholith in the Zambesi belt, Zimbabwe. Tectonophysics 138, 121–158.
Yeh, M.-W., Bell, T.H., 2004. Significance of dextral reactivation of an E-W transfer fault in the formation of the Pennsylvania orocline, central Appalachians. Tectonics 23 TC5009.